https://doi.org/10.5194/amt-2020-348
Preprint. Discussion started: 17 October 2020

Atmospheric Measurement Techniques Discussions

Measurements of CFC-11, CFC-12, and HCFC-22 total columns in the atmosphere at the St. Petersburg site in 2009-2019

Alexander Polyakov, Anatoly Poberovsky, Maria Makarova, Yana Virolainen, and Yuri Timofeyev
St. Petersburg State University, 7–9 Universitetskaya Emb., St. Petersburg 199034, Russia
Correspondence: Alexander Polyakov (a.v.polyakov@spbu.ru)

Abstract. The retrieval strategies for deriving the atmospheric total columns (TCs) of CFC-11 (CCl_3F), CFC-12 (CCl_2F_2), and HCFC-22 ($CHClF_2$) from ground–based measurements of IR solar radiation have been improved. We demonstrate the advantage of using the Tikhonov–Phillips regularization approach for solving the inverse problem of the retrieval of these gases and give the optimized values of regularization parameters. The estimates of relative systematic and random errors amount to 7.61 % and 3.08 %, 2.24 % and 2.40 %, 5.75 % and 3.70 %, for CFC-11, CFC-12, and HCFC-22, respectively. We analyze the time series of the TCs and mean molar fractions (MMFs) of CFC-11, CFC-12, and HCFC-22 measured at the NDACC site St. Petersburg located near Saint Petersburg, Russia for the period of 2009–2019. Mean values of the MMFs for CFC-11, CFC-12, and HCFC-22 total 225, 493, and 238 pptv, respectively. Estimates of the MMFs trends for CFC-11, CFC-12, and HCFC-22 account for $-0.40 \pm 0.07\,\%\,\mathrm{yr}^{-1}$, $-0.49 \pm 0.05\,\%\,\mathrm{yr}^{-1}$, and $2.12 \pm 0.13\,\%\,\mathrm{yr}^{-1}$, respectively.

We have compared the mean values, trends and seasonal variability of CFC-11, CFC-12, and HCFC-22 MMFs measured at the St. Petersburg site in 2009–2019 to that of 1) near–ground volume mixing ratios (VMRs) measured at the observational site Mace Head, Ireland (GVMR); 2) the mean in the $8-12$ km layer VMRs measured by ACE–FTS and averaged over $55-65°$ N latitudes (SVMR); and the MMFs of the Whole Atmosphere Community Climate Model for the St. Petersburg site (WMMF).

The means of the MMFs are less than that of the GVMR for CFC-11 by 9 pptv(3.8 %), for CFC-12 by 24 pptv(4.6 %); for HCFC-22, the mean MMFs does not differ significantly from the mean GVMR. The absolute value of the trend estimates of the MMFs is less than that of the GVMR for CFC-11 (-0.40 vs $-0.53\,\%\,\mathrm{yr}^{-1}$) and CFC-12 ($-0.49$ vs $-0.59\,\%\,\mathrm{yr}^{-1}$); the trend estimate of the HCFC-22 MMFs does not differ significantly from that of the GVMR. The seasonal variability of the GVMR for all three gases is much lower than the MMFs variability.

The means of the MMFs are less than that of the SVMR for CFC-11 by 10 pptv (4.3 %), for CFC-12 by 33 pptv (6.3 %), and for HCFC-22 by 2 pptv (0.8 %). The absolute value of the trend estimates of the MMFs is less than that of the SVMR for CFC-11 (-0.40 vs $-0.63\,\%\,\mathrm{yr}^{-1}$) and CFC-12 ($-0.49$ vs $-0.58\,\%\,\mathrm{yr}^{-1}$); the trend estimate of the HCFC-22 MMFs does not differ significantly from that of the SVMR. The MMF and SVMR values show nearly the same qualitative and quantitative seasonal variability for all three gases.

The means of the MMFs are greater than that of the WMMF for CFC-11 by 22 pptv (10 %), for CFC-12 by 15 pptv (3.1 %), and for HCFC-22 by 23 pptv (10 %). The absolute value of the trend estimates of the MMFs is less than that of the WMMF for CFC-11 (-0.40 vs $-1.68\,\%\,\mathrm{yr}^{-1}$), CFC-12 ($-0.49$ vs $-0.84\,\%\,\mathrm{yr}^{-1}$), and HCFC-22 ($2.12\,\%\,\mathrm{yr}^{-1}$ vs $3.40\,\%\,\mathrm{yr}^{-1}$). The

https://doi.org/10.5194/amt-2020-348
Preprint. Discussion started: 17 October 2020


Atmospheric Measurement Techniques Discussions

MMFs and WMMF values show nearly the same qualitative and quantitative seasonal variability for CFC-11 and CFC-12, whereas the seasonal variability of the WMMF for HCFC-22 is essentially less than that of the MMFs.

In general, the comparison of the MMFs with the independent data shows a good agreement of their means within the systematic error of considered measurements. The observed trends over the St. Petersburg site demonstrate the smaller decrease rates for CFC-11 and CFC-12 TCs than that of the independent data, and the same decrease rate for HCFC-22. The suggested retrieval strategies can be used for analysis of the IR solar spectra measurements using Bruker FS125HR spectrometers, e.g. at other IRWG sites of the NDACC observational network.

Copyright statement. TEXT

1 Introduction

Since the middle of the 20th century, anthropogenic trace gases, the molecules of which contain halogens, due to their specific physical and chemical properties have been actively used in climatic and refrigeration industry as well as in various propellants. Molina and Rowland (1974) have shown that these gases play an important role in the depletion of the stratospheric ozone. In particular, the photolysis of CCl_3F (trichlorofluoromethane, CFC-11) and CCl_2F_2 (dichlorodifluoromethane, CFC-12) in the stratosphere leads to the appearance of the active chlorine which is involved in ozone depletion reactions.

Although the major content of these gases is concentrated in the troposphere, in the equatorial region the global circulation moves them out to the lower and middle stratosphere. Then they are transported to the stratosphere of high–latitude regions where the destruction of the ozone layer results up to the appearance of so–called ozone holes. The WMO (2018, Appendix A) estimates the ozone depletion potential (ODP) of CFC-12 as $0.73 - 0.81$ (ODP of CFC-11, chosen as a reference, equals 1).

As the result of the Montreal Protocol and its amendments and adjustments that restricted the emission of chlorofluorocarbons (CFCs) (see (WMO, 2018)), the industry moved away from CFCs to less ozone–depleting hydrochlorofluorocarbons (HCFCs), especially $CHClF_2$ (chlorodifluoromethane HCFC-22). Although the ODP of HCFC-22 is much lower than that of CFCs, it is an ozone-depleting substance, too. Ozone depletion by HCFC-22 is primarily associated with the heating of the stratosphere, and its ODP, although small, totals 0.024–0.34.

CFC-11 and CFC-12, like HCFC-22, also absorb the infrared radiation, therefore they are all greenhouse gases. The Global Warming Potential (GWP) represents the integrated radiative forcing (RF) for a conditional time horizon ($20, 100, 500$ years) caused by the emission of a unit mass of a gas relative to the same RF value of CO_2 that is chosen as a reference for estimating the GWP of other gases. According to WMO (2018, Appendix A), the GWPs for 100 years are 5160 for CFC-11, 10300 for CFC-12, and 1780 for HCFC-22. One of the reasons of the high values of the GWP of these gases is their long lifetimes: $52, 102, 11.9$ years, respectively. Due to their long lifetimes, these gases are also good indicators for studying the transport and mixing processes in the upper troposphere and lower stratosphere (e.g. Hoffmann and Riese, 2004).

https://doi.org/10.5194/amt-2020-348
Preprint. Discussion started: 17 October 2020


Atmospheric Measurement Techniques Discussions

Since Molina and Rowland (1974) have reported that CFCs accumulated in the Earth's atmosphere lead to an increased rate of ozone depletion, the attention of both scientists and policymakers to the ozone hole problem has been increasing. Detecting and monitoring the ozone and other stratospheric gases as well as the ozone depleting substances including CFCs are crucial for testing the theories of the ozone hole formation mechanism (Cracknell and Varotsos, 2009).

The Montreal Protocol came into force in 1989 and stopped the using of CFC-11 and CFC-12, therefore their content in the atmosphere was declining at an average rate of 0.7–1.2 and 0.4–0.5 % per year, respectively (Brown et al., 2011). Having been accumulated in the troposphere, CFC-11 still provides a quarter of all chlorine reaching the stratosphere. The time needed for recovery of the ozone layer depends on the sustainability of the reduction in the concentration of CFC-11, CFC-12 and other freons in the atmosphere.

Based on the 2015–2017 data, Montzka et al. (2018) have shown that the rate of change in the CFC-11 atmospheric content decrease by approximately half to $-0.4\,\%\,\mathrm{yr}^{-1}$, assuming that this slowdown is caused by the emergence of new unregistered sources. This finding increases the importance of monitoring the atmospheric content of CFC-11. The maximum of the CFC-12 atmospheric content has been observed in the early 2000s, since then its steady decrease is detected with an average rate of 0.4–0.5 % per year (AGAGE network, http://agage.mit.edu/data/agage-data). As HCFCs are the 'transitional substances' for the replacement of CFCs, their production has increased rapidly in developed countries in the 1990s and peaked in the mid–1990s. In the 2000s, the production and consumption of HCFCs in developed countries have decreased as a response to the Montreal Protocol. Meanwhile, in developing countries the production and consumption of HCFCs have increased rapidly in the 2000s and have not been controlled until 2016. The Kigali Amendment to the Montreal Protocol on Substances that Deplete the Ozone Layer has come into force on 1 January 2019, following ratification by 65 countries. Under the Amendment, all countries will gradually phase down HCFCs by more than 80 percent over the next 30 years and replace them with more environmentally friendly alternatives.

Until recently, two data sources were mainly used to study the trends and seasonal variations of the considered gases: local measurements of near ground concentrations (for example, the AGAGE networks Dunse et al. (2005), and NOAA's Halocarbons & other Atmospheric Trace Species Group NOAA CAMP Montzka et al. (1993)) and satellite limb measurement experiments ILAS, ACE–FTS, MIPAS (Hoffmann et al., 2008; Mahieu et al., 2008; Eckert et al., 2016; Kellmann, et al., 2012; Boone et al., 2020). In contrast to satellite and in situ measurements near ground, ground–based IR measurements of the solar radiation are sensitive to the total columns (TCs) of atmospheric gases up to the Earth's surface. This method complements the information obtained by the first two methods, although it does not allow getting the detailed information on the vertical gas distribution.

Previously, Fourier transform infra red (FTIR) measurements of freons TCs were rather episodic (e.g. Notholt, 1994; Zander et al., 2005; Mahieu et al., 2010), although they started to be used more actively in the last decade (e.g. Mahieu et al., 2013, 2017; Zhou et al., 2016; Prignon et al., 2019). Within the NDACC network (http://www.ndsc.ncep.noaa.gov), regular FTIR measurements provide the information on the TCs of a number of atmospheric trace gases, including freons, with a large spatial coverage (at 19 out of 77 network stations located at latitudes between 78° S to 80° N). Mahieu et al. (2017) reported on the results of R-142b measurements along with the comparison with independent data and the trend estimates. Zhou et al.

https://doi.org/10.5194/amt-2020-348
Preprint. Discussion started: 17 October 2020


Atmospheric Measurement Techniques Discussions

(2016) showed the results of CFC-11, CFC-12, and HCFC-22 measurements at two NDACC sites on Réunion Island for the period of 2004–2016, including the trend estimates and the comparison with the satellite data. Prignon et al. (2019) proposed a technique for estimating the TCs of HCFC-22 at the Jungfraujoch mountain station and corresponding time series of HCFC-22 TCs for 1999-2018 along with the trend analysis for various time periods.

The archive of ground–based spectroscopic measurements of IR solar radiation performed at the NDACC site St. Petersburg (Timofeyev et al., 2016; Virolainen et al., 2017) since 2009 can be used to derive the data on TCs of CFC-11, CFC-12, and HCFC-22. First in Russia estimates of the CFC-11 TCs using the FTIR method and the original retrieval technique were given by Yagovkina et al. (2011). Polyakov et al. (2018) presented the preliminary results of the CFC-11, CFC-12, and HCFC-22 TCs retrieval for the period of 2009-2016 using the SFIT4 software, version 0.9.4.4, described by Hase et al. (2004). It should be noted that the SFIT4 software is a versatile tool, and it is necessary to customize it for a specific task through a selection of numerous parameters. Polyakov et al. (2018) selected these parameters based on the studies at other NDACC sites (Mahieu et al., 2010; Zhou et al., 2016) and the general recommendations of the IR working group (IRWG) of the NDACC network. However, these first results raised a number of questions, in particular, an unreasonably large scatter of the TCs values and significant seasonal variations. Later study showed that the observed scatter and seasonal variability were not due to objective reasons, but to peculiarities of the processing retrieval technique. The difficulties of the freons TCs retrievals are caused, first of all, by small values and a smoothed spectral dependency of the radiation absorption by these gases which lead to the low information content of the FTIR measurements with respect to the freons TCs.

Later on, the retrieval techniques for estimating the CFC-11, CFC-12, and HCFC-22 TCs by the FTIR method at the St. Petersburg site were refined and improved. These techniques were described in detail by Polyakov et al. (2019a, b, 2020a). In the current study, we improve the developed retrieval methods by using the Tikhonov–Phillips (T–Ph) approach which is more suitable for long–lived gases with a pronounced trend. We present the main features of the developed techniques and analyze the use of the T–Ph approach. The time series of CFC-11, CFC-12, and HCFC-22 TCs are extended until the fall of 2019. The derived time series of the TCs are analyzed and compared to the independent measurements and numerical modeling data.

2 Technique for inverting the spectroscopic measurements

2.1 Spectroscopic measurements

The main features of the ground–based station, observational system and the technique for measuring the solar spectra used in this study are described in detail by Timofeyev et al. (2016).

The St. Petersburg site is located in Peterhof, $30\,\mathrm{km}$ west of St. Petersburg city. The geographical latitude of the site $59.88^\circ\,\mathrm{N}$ predetermines winter measurements with a low Sun elevation: in December–January, the maximum height of the Sun does not usually exceed 20°; spectroscopic measurements are performed up to the Sun's height of 5°. Due to peculiarities of the local weather, measurements are mainly ($76\,\%$) carried out in spring and summer seasons. The analyzed spectra are obtained without any additional apodization of the interferograms, their spectral resolution is $0.005\ \mathrm{cm}^{-1}$. The observational system is based on a Bruker FS125HR Fourier spectrometer, but some of the equipment is non–standard. In particular, before February 2016

https://doi.org/10.5194/amt-2020-348
Preprint. Discussion started: 17 October 2020


Atmospheric Measurement Techniques Discussions

a non–standard spectral filter F3 was used for measurements in the spectral region with considered freons absorption bands. Since this filter was plane–parallel, a parasitic interference arose in it, leading to the appearance of a periodic quasi–harmonic noise component (QHN).

The period of the QHN is caused by the material and the thickness of the filter, and in the spectral region $800 - 900\,\mathrm{cm}^{-1}$ it is close to $1.1\,\mathrm{cm}^{-1}$, while the amplitude of the QHN varies from zero to a few percent value depending on random filter positioning parameters. To analyze the presence and the amplitude of the QHN, we perform the Fourier analysis in the most transparent spectral range $892 - 905\,\mathrm{cm}^{-1}$ for harmonic components with periods in the intervals of $1 - 1.25\,\mathrm{cm}^{-1}$. The QHN amplitude is calculated relative to the mean signal value in this spectral range. The analysis of the Inverse Problem Solution Process (IPSP) shows that it is reasonable to exclude from consideration the spectra with the QHN amplitude that exceeds $2\ \%$. As a result of the described filtering, 2900 from 3350 (i.e. $86\ \%$) spectra measured before February 2016 have been selected for further processing. In February 2016, the F3 filter has been replaced by the standard IRWG NDACC filter f6 which wedge–shaped design eliminates the QHN.

For a preliminary assessment of the signal to noise ratio (SNR), the standard deviation (SD) of the signal is estimated in the opaque spectral range $660 - 680\,\mathrm{cm}^{-1}$, then the maximum signal value in the entire measured spectrum is divided by the obtained value. To exclude noisy spectra and possible non–linearity in measurements, we use only measurements with SNR values ranging from 50 to 600, the percentage of which is more than $98\,\%$, and typical SNR values are $300 - 500$.

2.2 Main parameters of the retrieval technique

In previous studies, Polyakov et al. (2019a, b, 2020a) have determined a number of parameters of the retrieval strategy using the SFIT4 code for deriving the TCs of the studied gases from the FTIR measurements at the St. Petersburg site: the boundaries of microwindows, the mean/apriori profiles of the measured gases, the magnitude and variability of the zero level, periods for taking into account (or excluding) the QHN, and the shape of the spectrum baseline (SBL). In those studies, the main criterion for choosing the optimal values of setup parameters was the stability of the target gas TCs during a day. More precisely, the root mean square value (RMS) over all days for SD of the gas TCs per a day was minimized. Along with the daily variability of the TCs, the mean value and the SD of the information content of measurements (degrees of freedom for signal, DFS) (Rodgers, 2000, p. 19) as well as the estimates of the systematic and random measurement errors and the spectral residual — the RMS difference between measured and calculated spectra for the retrieved state of the atmosphere (χ^2) were also analyzed. Table 1 presents the main optimized parameters obtained in previous studies.

https://doi.org/10.5194/amt-2020-348
Preprint. Discussion started: 17 October 2020

Atmospheric Measurement Techniques Discussions

Table 1. The main parameters of the inversion of the spectra for deriving the TCs of freons obtained by Polyakov et al. (2019a, b, 2020a).

Gas	Microwindow, cm^{-1}	Other gases	H_2O spectroscopy	Accounting for QHN (beam)
CFC-11	830–860	H_2O(profile), CO_2, O_3, HNO_3, $COCl_2$ (columns)	HITRAN 2016	$1.12\,cm^{-1}$ before 2016
CFC-12	1160–1162	H_2O, O_3, N_2O, CH_4 (columns)	HITRAN 2009	$1.26\,cm^{-1}$ before 2016
HCFC-22	828.75–829.4	CO_2, O_3, H_2O (columns)	HITRAN 2009	$1.1\,cm^{-1}$ before 2016

While processing the measured spectra, the spectroscopic parameters supplied as a part of the SFIT-4 software are used. Target gas absorption is calculated based on pseudo–lines (see mark4sun.jpl.nasa.gov/pesudo.html for pseudo–lines), interfering gases absorption is calculated based on spectroscopic information from the HITRAN database which is described in detail by Polyakov et al. (2019a, b, 2020a). The apriori information on the physical state of the atmosphere is taken from the NCEP CPC (presented on ftp.cpc.ncep.noaa.gov/ndacc/ncep); water vapor profiles used in the retrieval are independently derived from the FTIR measurements, the technique is described by Virolainen et al. (2017). The apriori profiles of other interfering gases are taken from the Whole Atmosphere Community Climate Model (WACCM). As a first guess for target gases, the mean profiles of the WACCM dataset for the 2009–2019 period are used. The using of a wide spectral window for CFC-11 retrieval ($30\,cm^{-1}$, see Table 1) is unusual for deriving the information on the gas content from the high resolution IR spectra and requires the non-standard approach. This approach was described in detail by Polyakov et al. (2020a); the main features of this approach are listed below.

The main factor that determines the shape of the SBL is the filter spectral transmission function (STF). We have measured the STF in a special experiment using an artificial light source. Water vapor continuum makes a significant contribution to radiation attenuation (Mlawer et al., 2012). Our calculations have shown that its contribution in the considered spectral region under conditions of the St. Petersburg site can significantly exceed $50\,\%$. For a $30\,cm^{-1}$ window, the selectivity of continual uptake is sufficient to influence the IPSP results. To calculate the water vapor continuum, we use a free–distributed computer code (MT_CKD, 2017) and the daily profiles of water vapor independently derived from the FTIR measurements (Virolainen et al., 2017).

Repeated measurements of the STF show that over time they exhibit a specific spectrum of absorption by amorphous ice (e.g. Hudgins, et al., 1993; Lynch, 2006) formed at the temperatures that has a receiver cooled by liquid nitrogen (hereinafter referred to as cryo–sediment). The absorption of radiation by the cryo–sediment depends on its thickness which increases during the measurement period and decreases during the period of inactivity of the instrument when the receiver is not cooled. In addition, the water vapor from the atmospheric air gradually (on a monthly scale) seeps into the evacuated zone of the instrument and also leads to an increase of the cryo–sediment thickness. To compensate for its variability, the SBL shape is refined with the second–degree wavenumber polynomial implemented in the SFIT4 code. With turning on one more variable, the correction of the SBL curvature specified by the coefficient at the second power of the wavenumber (hereinafter – curvature value) can lead to "overfreedom" of the solution. To avoid this, the apriori curvature value uncertainty is limited. The parameters for

https://doi.org/10.5194/amt-2020-348
Preprint. Discussion started: 17 October 2020


Atmospheric Measurement Techniques Discussions

compensating the SBL shape due to absorption by the cryo–sediment are selected in two steps. On the basis of a series of IPSP calculations minimizing the daytime variability of the CFC-11 TCs, the apriori thickness of the cryo-sediment and the apriori curvature value uncertainty are selected. The apriori curvature value is chosen to be 0. The main components of accounting for the SBL shape are shown in Table 2.

Table 2. Parameters that determine the shape of the SBL for CFC-11.

Accounting for cryo–sediment		Filter accounting (2 different functions for F3 and f6)	Continuum preliminary calculation
Apriori thickness	variability		
0.3 µm for F3, 0.9 µm for f6	Curvature fitting: A priori 0, uncertainty 10^{-6}		

2.3 Method for solving the inverse problem

In earlier studies, Polyakov et al. (2018) used an optimal estimation method (OE) (Rodgers, 2000, p. 65) for solving the inverse problem, i.e. apriori information was given in the form of a mean profile and a covariance matrix built on the basis of the WACCM dataset (Park et al., 2013) for the period of 2009–2019. In accordance with WMO (2018), all three considered gases are characterized by a long lifetime, therefore the low variability of their content on a time scale of less than several years is expected and confirmed, for example, by measurements of AGAGE and HATS networks (Dunse et al., 2005; Montzka et al., 1993). In this case, their long–term variability turns out to be predominant. Such a character of the variability, especially in combination with a small DFS (e.g. Zhou et al., 2016; Polyakov et al., 2019a, b, 2020a), is better described by a priori information of the Tikhonov–Phillips approach presented by Tikhonov (1963) and Phillips (1962). Unlike the OE, the T–Ph approach does not "pull" the solution to the mean profile but only limits its vertical variability. The use of the first order T–Ph regularization (Tikhonov, 1963) in retrieving the TCs of trace gases is described in detail, for example, by Sussmann et al. (2011). Besides, when choosing the type of the apriori information (OE or T–Ph), it should be taken into account that the OE approach requires the use of the covariance matrices for describing the variability of the target gases profiles, preferably the real covariance matrices, that are unavailable for the considered freons. Therefore we chose the T–Ph regularization for spectra inverting.

For opimization of the regularization parameter α, we use a technique based on minimizing the daily variability of the TCs suggested by Sussmann et al. (2011). In addition, we analyze the spectral residual RMS, sometimes denoted as (χ^2) , and the values of DFS. For analysis of the regularization parameter, we use spectroscopic measurements in 2017 which are characterized by a fairly stable quality of measurements, a low noise level, and a possibly more uniform distribution of measurements throughout the year including the winter months. The choise of 2017 has also been made due to the measurements with the f6 filter which is currently used by other sites of the IRWG NDACC network. The testing calculations for filter F3 have been carried out for 2015, and they confirm that the values of α obtained for 2017 for f6 filter are also optimal for F3 filter.

https://doi.org/10.5194/amt-2020-348
Preprint. Discussion started: 17 October 2020

Atmospheric Measurement Techniques Discussions

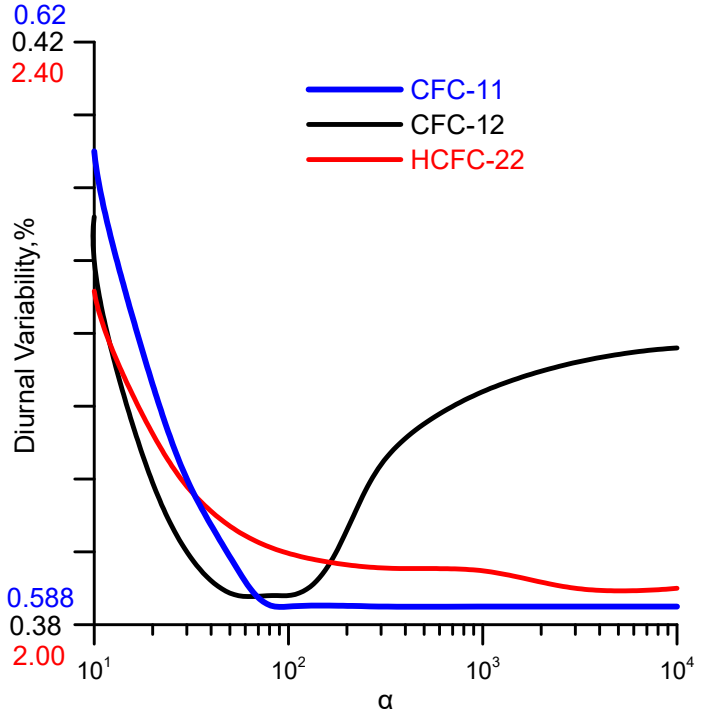

Figure 1. Dependence of the TCs daily variability on the regularization parameter α.

Figure 1 depicts the RMS daily variability of the TCs of studied gases as a function of α for 2017. For CFC-11, the minimum of the daily variability of $0.589\,\%$ is reached asymptotically for all values of α not less than 85, and the DFS at $\alpha = 85$ differs from 1 (DFS$= 1.08$). For CFC-12, the optimal value of the regularization parameter $\alpha = 85$, this value corresponds to the daily minimum of $0.382\,\%$, and DFS totals 1.18. For HCFC-22, the minimum of daily variability of $0.398\,\%$ is reached asymptotically for all values of α, starting from 3×10^3, the DFS for all these values amounts to 1.00, and the both parameters do not change for α greater than 3×10^3. This can be interpreted as the complete absence of the information on the vertical

https://doi.org/10.5194/amt-2020-348
Preprint. Discussion started: 17 October 2020

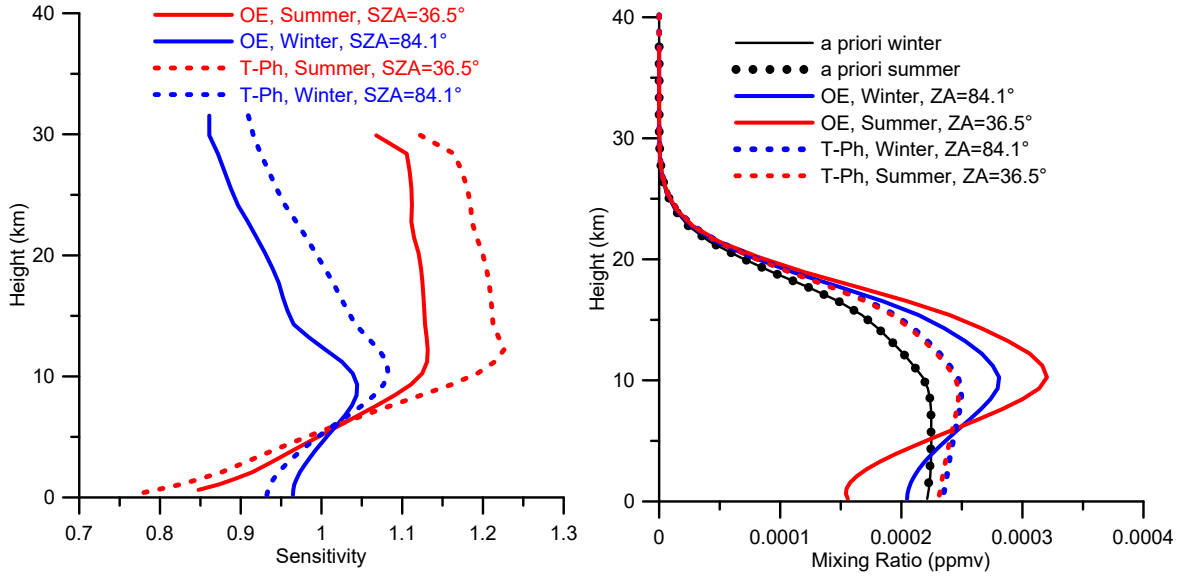

Figure 2. Sensitivity of CFC-11 TCs to variation of its VMR profile (left) and a priori and retrieved profiles (right) on 16 June 2018 09:54 (red) and 14 October 2018 13:57 (blue).

profile of HCFC-22 in spectral measurements, i.e. only the information on the first guess profile multiplier. We performed the retrieval for both the multiplier and the T–Ph approach with $\alpha = 3 \times 10^3$. It turns out that although the SFIT4 software gives practically the same results, the option with the multiplier retrieval does not allow calculating the error budget. Therefore, we use the T–Ph method for HCFC-22 retrieval with $\alpha = 3 \times 10^3$.

It should be noted that the target parameter of the retrieval, TC, is calculated from the initially retrieved vertical profile of the gas. Therefore, it is important to control the retieval of trace gases profiles. For all three considered gases, figures 2–4 depict the sensitivity functions of the TCs to relative variations in the gases profile at different heights (left) (see about averaging kernel (AK) area (Rodgers and Connor, 2003)) and the examples of initial (first guess) and retrieved volume mixing ratio (VMR) profiles (right). All curves are shown for two typical measurements: in a fall–winter season with a low Sun elevation and a low humidity, and in summer, with a high for the site latitude Sun elevation and a wet atmosphere. All parameters in the figures are given for a regularization of both the OE and the T–Ph methods.

https://doi.org/10.5194/amt-2020-348
Preprint. Discussion started: 17 October 2020

Atmospheric Measurement Techniques Discussions

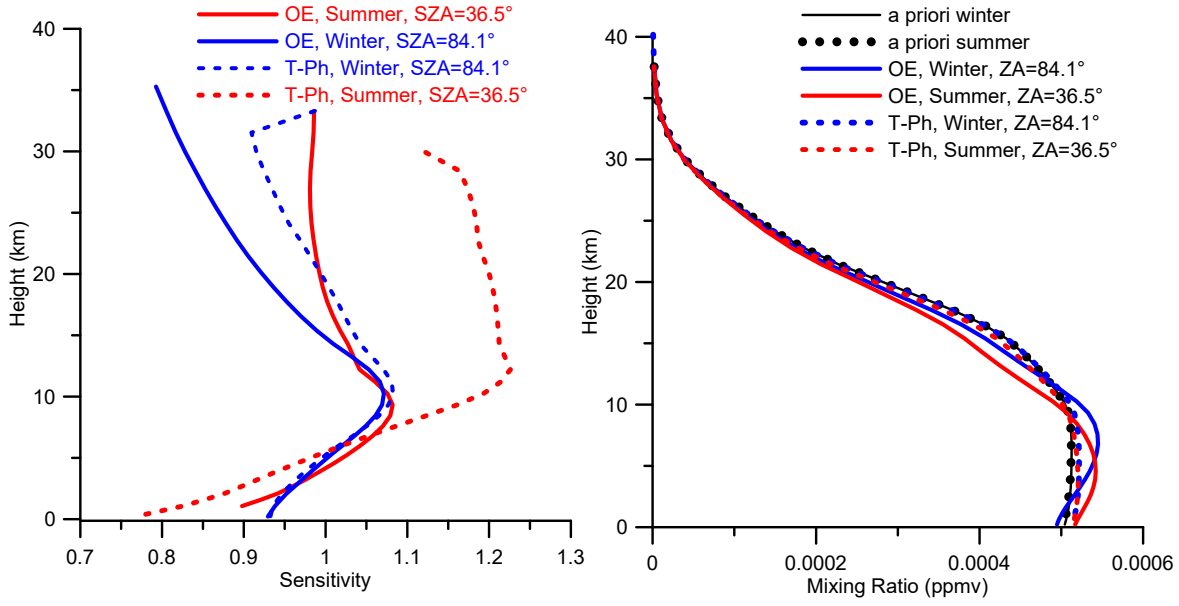

Figure 3. Sensitivity of CFC-12 TCs to variation of its VMR profile (left) and prior and retrieved profiles (right) on 16 June 2018 09:54 (red) and 14 October 2018 13:57 (blue).

Figures 2–4 demonstrate that the sensitivity, which for the ideal case should be equal to 1 at all heights, turns out to be noticeably lower (from 0.5 to 0.8 for different gases, seasons and methods) at the surface. Then sensitivities increase, reaching a maximum at heights of $8-12\,\mathrm{km}$ for CFC-11 and CFC-12, and at heights above $12\,\mathrm{km}$ for HCFC-22 which is due to a higher stratospheric content of the latter. Above, the sensitivity decreases which can no longer be significant due to the fall of the VMR of the considered gases. The consequence of this is an underestimation of the variations in the gas profile at the surface and a significant distortion of the profile shape for all three gases when using the OE method. For the T–Ph method, although the sensitivity at the surface is less than that for the OE, such a distortion of the profile shape does not occur since the prior information does not require the solution to be close to the apriori profile. Therefore, the profiles retrieved by the OE method are less reliable for the long–lived gases well mixed in the troposphere, and an advantage of the choice of the T–Ph method to solve the inverse problem is confirmed. As seen from Fig. 2–4, the measurement conditions have a significant effect on the sensitivity functions. In winter, when the Sun elevation is low corresponding to a thicker atmosphere in the solar beam path and low water vapor content, the information content of measurements is higher than in summer. For all three gases, the

https://doi.org/10.5194/amt-2020-348
Preprint. Discussion started: 17 October 2020

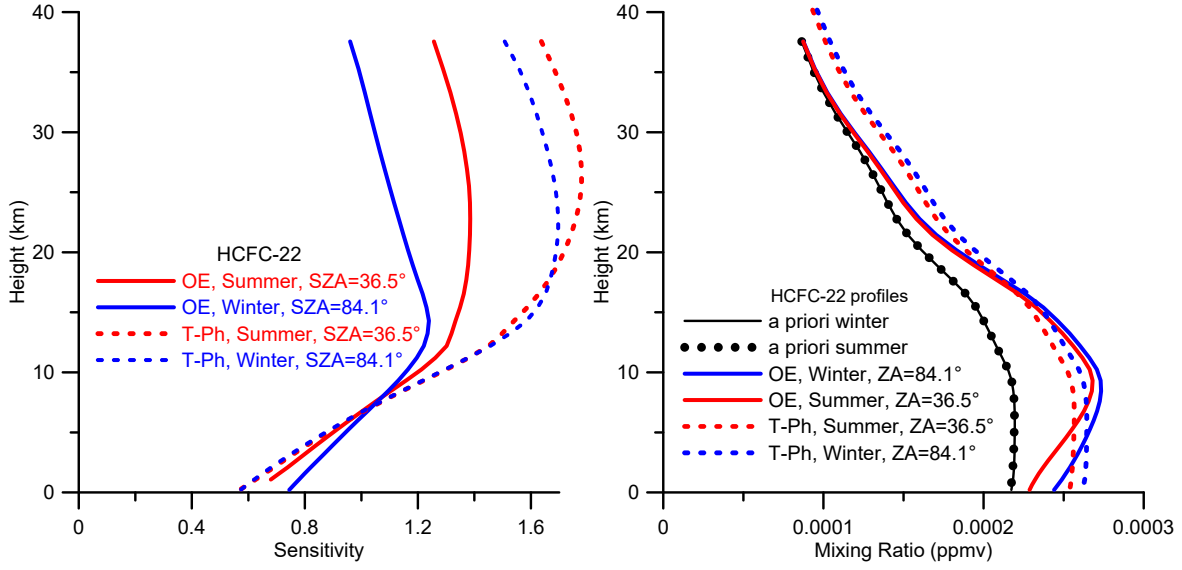

Figure 4. Sensitivity of HCFC-22 TC to variation of its VMR profile (left) and prior and retrieved profiles (right) on 16 June 2018 09:54 (red) and 14 October 2018 13:57 (blue).

sensitivity is far from the unit at a greater extent in the lower troposphere in high humidity conditions in summer. Using T–Ph apriori information and choosing the regularization parameter based on minimizing the daily variability of TCs, we obtained $DFS = 1$ for HCFC-22; the DFS value of other two gases is close to 1 (1.05 and 1.20, see Table 4). Prignon et al. (2019) reported the higher values of DFS (DFS = 1.97) caused by another regularization method and a low atmospheric water vapor content above the mountain (3580m a.s.l) site Jungfraujoch. Prignon et al. (2019) used the OE regularization, and in this case the DFS values turned out to be noticeably higher than for the T–Ph regularization.

3 Results and analysis

The techniques described above were applied to processing the entire archive of spectral measurements at the NDACC site St. Petersburg for the period of 2009–2019.

https://doi.org/10.5194/amt-2020-348
Preprint. Discussion started: 17 October 2020


Atmospheric Measurement Techniques Discussions

3.1 The filtering of the results

Table 3 presents a number of statistical characteristics and the assessment of the total errors of the obtained TCs of the studied gases.

Table 3. Summary of the statistics for retrieved freons TCs before filtering. The numbers after the "±" sign indicate the standard deviation of the values.

N	Parameter	CFC-11	CFC-12	HCFC-22
1	Number of spectra/days	4773/720	4768/718	4585/714
2	RMS, %	0.529 ± 0.460	0.447 ± 0.546	0.399 ± 0.286
3	Total Systematic Error, %	7.60 ± 0.18	2.26 ± 0.16	5.75 ± 0.08
4	Total Random Error, %	3.23 ± 0.77	2.56 ± 0.94	4.18 ± 2.66
5	Daily SD, %	1.354	0.704	5.63
6	DFS	1.07 ± 0.09	1.20 ± 0.05	1.00 ± 0.00

The first row in Table 3 shows the total number of spectra / days for which the TCs have been obtained. These numbers are different for different gases since the inverse problem solution algorithm implemented in SFIT4 does not always provide a solution. The total number of spectra suitable for processing for over more than 10 years of observations (from March 2009 to August 2019) is about 4500–4800, and they have been measured for about 720 days. Thus, on average, the FTIR measurements at the St. Petersburg site are carried out for 68 days per year. Such a relatively low annual frequency of the measurement days number is primarily due to the geographical latitude and climatic features of the site.

As we observe some outliers in the HCFC-22 TCs time series before 2016, we discard the TCs values that differ from the approximating line (trend) by more than 3 SD values. On the next step we filter the retrieved TCs using the following criteria: the deviation from the mean statistical characteristics presented in Table 3 should not be greater than 2×SD.

Table 4 gives a summary of the measurement statistics (rows 1–7) and the error budget (rows 8 – 18) of the retrieved TCs. The general information on the analyzed spectra is given in row 1 (the number of measurement days and single measurements) and in row 2 (the spectral residuals). The number of days is close to 670 and the number of the retrieved TCs is close to 3900 for each gas. The spectral residual is the most important parameter of the inverse task solving; it characterizes the quality of fitting the measured spectra by calculated one. Ideally, the spectral residual should be equal to the measurements noise level. For considered gases, the mean values of the spectral residuals vary from 0.34 to $0.52\,\%$ depending on the gas; it corresponds to the SNR values of $209, 280$, and 327 for CFC-11, CFC-12, and HCFC-22, respectively. Comparing these values to the preliminary determined SNR in the opaque spectral range ($364, 351$ and 324, in the same order of gases), we see that for CFC-11 and CFC-12 they are slightly less and for HCFC-22 are nearly the same. This means that for CFC-11 and CFC-12 the used radiative transfer model and a set of parameters, although satisfactory, but not ideally describe the absorption of radiation by the atmosphere and the observational system, whereas for HCFC-22 the retrieval technique works in the best way.

https://doi.org/10.5194/amt-2020-348
Preprint. Discussion started: 17 October 2020


Atmospheric Measurement Techniques Discussions

The SFIT4 software allows to calculate an error budget based on the Rodgers (2000, Chapt. 3) approach for each measurement. Rodgers (2000, Eq. 3.16) considers 4 components of the measurement error: the smoothing error, model parameter error, forward model error, and the retrieval noise. To estimate the smoothing error, it is necessary to have real covariance matrices of the gas vertical profiles, which are not available, therefore we cannot estimate this component of the error. We can only assume that it is small, because due to their long lifetime, we expect constant VMR profiles of the considered gases in the troposphere. The model parameter error is caused by the inaccuracies in setting the parameters describing the instrument and the state of the atmosphere.

To calculate the terms of the model parameter error, which are shown in rows 8–14 of Table 4, equation (Rodgers, 2000, Eq. 3.18) is used. For this equatuon, it is necessary first to set the uncertainties of various parameters which are taken into account. Rodgers (2000) enters them as elements of the S_b matrix, the corresponding column for these elements is presented in Table 4. For the temperature profile (row 8) below $40\,\mathrm{km}$, where the profiles of the considered gases are derived, the absolute value of the temperature systematic error totals $1-2\,\mathrm{K}$, random error totals $2-4\,\mathrm{K}$ depending on altitude. For other parameters, the relative errors are indicated in other rows of the Table.

In addition to the fixed parameters, two types of parameters are derived in the retrieval process: 1) the retrieval parameters including a number of instrumental parameters such as spectrum baseline (a slope for all three gases and a curvature for CFC-11), instrumental line shape, and QHN before 2016, and 2) the content of interfering atmospheric gases listed in Table 1 (column "other gases"), which absorption lines overlap with lines of the target gas. Their contribution to the errors of target gases TCs retrieval are shown in rows 15 (Interfering species) and 16 (Retrieval parameters).

The forward model error (Rodgers, 2000, Eq. 3.16) is considered to be negligible in our retrieval. The retrieval noise shown in row 17 indicates the error related to the spectra measurement noise.

A row 18 in Table 4 demonstrates that the total systematic errors of the TCs retrieval for CFC-11 and HCFC-22 are relatively large, amounting to 7.61 and $5.75\,\%$, and these values are almost entirely due to the uncertainty in the spectroscopic information on the intensities of the pseudo–lines (row 10 of Table 4). For CFC-12, the total systematic error is estimated at $2.2\,\%$, the main source of this error is the uncertainty of the temperature profile (row 8 of Table 4). Note that the value of the total systematic error is slightly variable, its SD is maximal for CFC-11 comprising for $0.16\,\%$. The total random error as well as its variability is maximal for HCFC-22. The main contribution to it is made by the spectral measurement error which is caused by the low absorption of the solar radiation by this gas. The random components of the total error for other two gases, 3.08 and $2.40\,\%$, are more stable and their main source is the error in the temperature profile (see row 8). It should be noted that the used filter has a significant effect on the errors and variability of the HCFC-22 TCs. When switching to the IRWG NDACC f6 filter in February 2016, the daily variability of the results (row 4 of Table 4) has decreased by 1.5 times, and the random component of the total error (row 18) has decreased by $1.4\,\%$, mainly due to the error of spectroscopic measurements.

Rows 3–7 of Table 4 present the characteristics of the target gases retrievals, TCs and mean molar fractions (MMFs). Row 3 shows the means, and row 4 shows the RMS daily variability of the results, which can be interpreted as their precision. Comparison of the latter values with the estimates of the random error demonstrates that for HCFC-22 the daily variability practically coincides with the total random error. This is due to the largest contribution of the measurement noise (row 17

https://doi.org/10.5194/amt-2020-348
Preprint. Discussion started: 17 October 2020


Atmospheric Measurement Techniques Discussions

of Table 4), which does not have a systematic component during a day, to the random error. The other two gases show a significantly different ratio, the daily variability is noticeably less than the random error – 0.76 vs $3.08\,\%$ for CFC-11 and 0.58 vs $2.40\,\%$ for CFC-12. This is due to the largest contribution of the temperature profile, which is variable during a day but is set as a daily averaged value, to the random error for these gases. Therefore, the random error has a significant component of a systematic nature during one day of measurements, but randomly changes from one day to another. It should be noted that the temperature profile changes insignificantly during a day, so the daily variability of the MMFs contains a related component and exceeds the contribution of a total random noise of spectroscopic measurements. Thus, the resulting error budget estimates and the daily variability of the results are mutually consistent.

The DFS (row 5) for all gases is close to 1 which is primarily due to the used apriori information of the T–Ph type of regularization and the selection of the regularization parameter α based on minimizing the daily variability of the gas TCs. Row 6 of Table 4 shows the value of the trend estimate. To assess the trend values, the methodology described by Gardiner et al. (2008) is used (see below) which is based on the RMS approximation of the gas concentration variability by a three–term segment of the Fourier series and bootstrap methods of confidential intervals assessment for $95\,\%$ probability. Finally, row 7 shows the RMS difference between the MMFs and the trigonometric Fourier series used to estimate their temporal variability. For CFC-11 and CFC-12, these values are close to the estimate of the random error (2.8 vs $3.08\,\%$ and 2.1 vs $2.40\,\%$) which indicates an adequate description of their variability by the Fourier series. At the same time, for HCFH-22, the RMS difference is $5.3\,\%$ which exceeds the random error of $3.7\,\%$, and the HCFC-22 variability contains some other components besides the trigonometric Fourier series.

https://doi.org/10.5194/amt-2020-348
Preprint. Discussion started: 17 October 2020

Atmospheric Measurement Techniques Discussions

Table 4. Summary of the statistics and the error budget for retrieved freons TCs after filtering (see the text). The relative uncertainties of spectroscopic parameters are $7, 1$ and 5% for CFC-11, CFC-12, and HCFC-22, respectively. S_b means a priori imprecision of parameters.

N	Parameter	CFC-11	CFC-12	HCFC-22
1	Number of spectra/days	$3864/678$	$3912/664$	$3855/663$
2	$RMS(\chi^2)$	0.524 ± 0.177	0.404 ± 0.161	0.344 ± 0.129
3	Mean TC, cm^{-2}(MMF, pptv)	$4.75 \times 10^{15}(225)$	$10.42 \times 10^{15}(493)$	$5.04 \times 10^{15}(238)$
4	Daily SD, %	0.76	0.58	$3.74(4.54/2.32)^*$
5	DFS	1.05 ± 0.06	1.20 ± 0.05	1.00 ± 0.00
6	Trend, $\%\ yr^{-1}$	-0.40 ± 0.07	-0.49 ± 0.05	2.12 ± 0.13
7	Total SD of MMF, % (except Fourier app.)	2.8	2.1	5.3

	Error , %	S_b, %	Systematic	Random	Systematic	Random	Systematic	Random
8	Temperature		2.29 ± 0.25	2.56 ± 0.30	1.96 ± 0.15	1.96 ± 0.12	1.72 ± 0.07	1.50 ± 0.06
9	SZA	0.1 ± 0.5	0.20 ± 0.17	1.03 ± 0.84	0.22 ± 0.18	1.09 ± 0.89	0.25 ± 0.25	1.27 ± 1.27
10	Target line intensity	$7/1/5$	7.02 ± 0.28		0.45 ± 0.49		5.04 ± 0.45	
11	Target temperature dependence of line width	$7/1/5$	0.00 ± 0.00				0.27 ± 0.05	
12	Target air broadening of line width	$7/1/5$	0.02 ± 0.03		0.61 ± 0.14		2.16 ± 0.24	
13	H2O spectroscopy	10	1.45 ± 0.57		0.31 ± 0.31		0.25 ± 0.35	
14	zshift	1 ± 1	1.03 ± 0.10	1.03 ± 0.10	0.12 ± 0.01	0.25 ± 0.03	0.10 ± 0.01	0.20 ± 0.02
15	Interfering species		0.04 ± 0.04		0.02 ± 0.01		0.19 ± 0.12	
16	Retrieval parameters		0.12 ± 0.07		0.02 ± 0.00		0.29 ± 0.05	
17	Spectra measurement noise			0.29 ± 0.13		0.20 ± 0.03		2.66±1.62 $(3.3/1.8)^*$
18	Total		7.61 ± 0.16	3.08 ± 0.36	2.24 ± 0.14	2.40 ± 0.54	5.75 ± 0.08	3.70 ± 1.29 $(4.32/2.92)^*$

*before / after February 2016

3.2 Analisys

Figures 5–7 show the results obtained in a form of the daily means of both the TCs and MMFs. The TC values directly represent the results of spectra inversion, while the MMFs calculated from the TCs allow to exclude the surface pressure variability and thus are more stable. To analyze the variability of the studied gases on the scale of both long–term trends and

https://doi.org/10.5194/amt-2020-348
Preprint. Discussion started: 17 October 2020


Atmospheric Measurement Techniques Discussions

seasonal variability, we use the approach implemented by Gardiner et al. (2008) for assessing the trends which is based on the approximation of a series of data by expansion in a finite–dimensional basis, Eq. (1).

$$F(t) \approx a + bt + c_1 f_1(t) + c_2 f_2(t) \ldots + c_k f_k(t) \tag{1}$$

In Eq. (1), $F(t)$ is the dependence approximated by the expansion, in our case represented by discrete measurement data, t – time (years), a – constant, b – linear term coefficient that is equal to trend value, $c_i, \quad i = 1, k$ – coefficients, k – number of the coefficients, $f_i(t)$ – basis functions. Due to the annual cyclical nature of atmospheric processes, a trigonometric Fourier series with a maximum period of a year is used which correspond to the basis functions (2)

$$f_{2i-1}(t) = cos(2\pi it), \qquad f_{2i}(t) = si(2\pi it), \qquad i = 1, m \tag{2}$$

for m = 3 or, which is the same, k = 6. Let us write Eq. (1) in the form (3), highlighting the nonlinear part S(t) (4) .

$$F(t) \approx a + bt + S(t) \tag{3}$$

$$S(t) = c_1 f_1(t) + c_2 f_2(t) \ldots + c_k f_k(t) \tag{4}$$

$S(t)$ can be considered as a periodic component of the measurement data time sequence and its one period can be analyzed as a seasonal data variability. Figures 5–7 in addition to the daily mean values of MMF and TC also show a dashed straight linear trend $a + bt$ and, with a solid black line, the result of approximating the measurement data by the trigonometric Fourier series (1), (2). Fig. 5 demonstrates a pronounced periodicity of the results, showing the seasonal variation of both TCs and MMFs of CFC-11. As it is shown below, a similar periodicity also manifests itself in satellite measurements and in the WACCM data. As expected, the MMFs exhibit a slightly smaller scatter than the TCs. Note that starting from April 2019, there is a sharp increase in the concentrations of CFC-11. At present, we have no way to explain whether such growth is objectively presented or caused by peculiarities in the operation of the device. At the same time, this growth noticeably affects the trend estimates. Therefore, when calculating the trends of the CFC-11 TCs and MMFs, we limit CFC-11 time series to April 2019, leaving the analysis of the reasons for this feature outside the scope of this study.

Analysis of the CFC-12 measurements (Fig.6) shows significantly different results. First of all, the comparison of Fig. 5 and 6 and estimates of the daily variability and measurement uncertainties of these gases demonstrate that the TCs and MMFs of CFC-12 show less scatter than that of CFC-11 except for some isolated anomalies. The seasonal variability of these values for CFC-12 is noticeably less than that of CFC-11. We also note that moving from TCs to MMFs, the deviations of the results from the approximating segment of the Fourier series decrease significantly. That is, variations in surface pressure and water vapor TCs make a significant contribution to the variability of the CFC-12 TCs which indicates small changes in its VMR profile. We will analyze these factors in detail in the next section.

Having considered the results of measurements of HCFC-22 daily means, we observe a large variability consistent with a large random component of the total error estimates (see Table 4). There are also noticeable seasonal variations. At first glance,

https://doi.org/10.5194/amt-2020-348
Preprint. Discussion started: 17 October 2020

Atmospheric Measurement Techniques Discussions

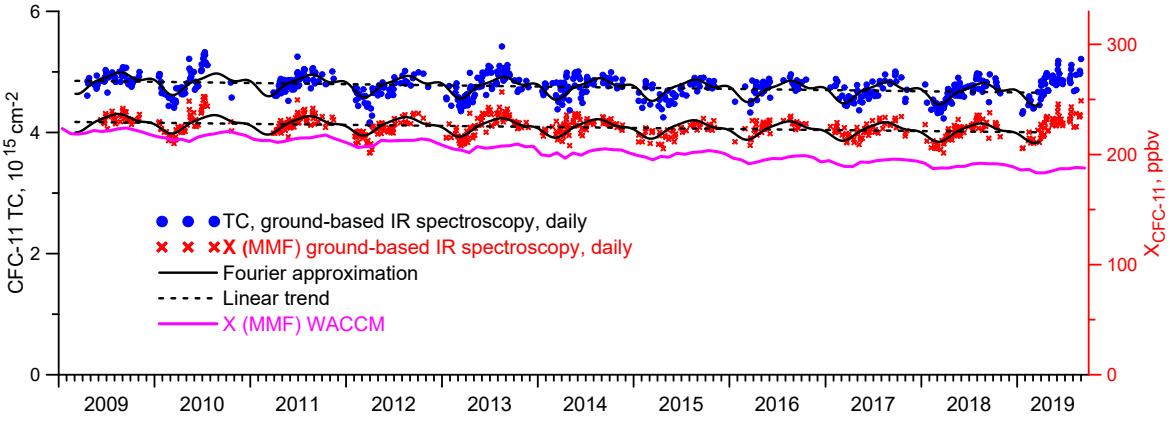

Figure 5. Daily mean TCs and MMFs of CFC-11. T–Ph parameter $\alpha = 85$.

the filter change in February 2016 clearly manifests itself in a change in the data scatter, but in 2016 the scatter looks no less than in previous years, sharply decreasing in 2017 and later. Noteworthy is the observed cessation of the increase in HCFC-22 values starting from 2018 previously described by Polyakov et al. (2020b). We also observe an increase in the scatter of the results in 2013 for all three gases due to the decrease in the SNR values mentioned in Section 2.1 for that year.

The use of harmonic expansion with a minimum period of 4 months correspondingly limits the elimination of seasonal fluctuations with a shorter period. Timofeev et al. (2020) used a different trend assessment method based on the exclusion of the seasonal variation by subtracting monthly mean values from the initial data which allowed to exclude features up to one month. Table 5 shows a comparison of the obtained results for the MMFs of the considered gases using two methods of trend estimation. The estimation of the width of the confidence interval of the trend value for the Gardiner et al. (2008) approach is carried out using the Bootstrap method, for the (Timofeev et al., 2020) method is calculated on the basis of the theoretical statistical approach.

https://doi.org/10.5194/amt-2020-348
Preprint. Discussion started: 17 October 2020

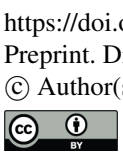

Atmospheric Measurement Techniques Discussions

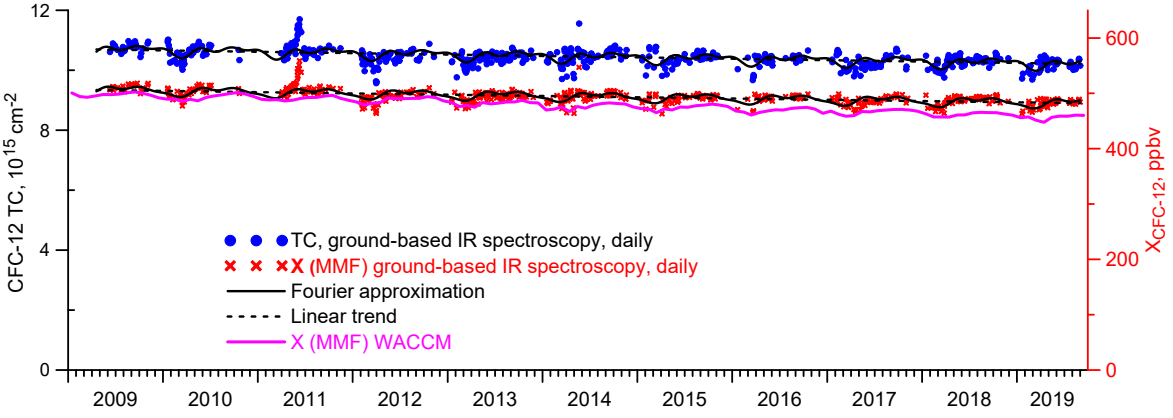

Figure 6. Daily mean TCs and MMFs of CFC-12. Filtered results, T-Ph parameter α=85.

Table 5. Estimated trends of the freon MMFs derived from the FTIR measurements at the St. Petersburg site in 2009–2019.

Gas	Gardiner et al (2008)	Timofeyev et al (2020)
CFC-11	-0.40±0.07	-0.39±0.08
CFC-12	-0.49±0.05	-0.46±0.05
HCFC-22	2.12±0.13	2.22±0.14

360 Table 5 demonstrates that the differences between two methods remain within the 95 % confidence intervals, i.e. are not significant.

https://doi.org/10.5194/amt-2020-348
Preprint. Discussion started: 17 October 2020

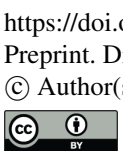

Atmospheric Measurement Techniques Discussions

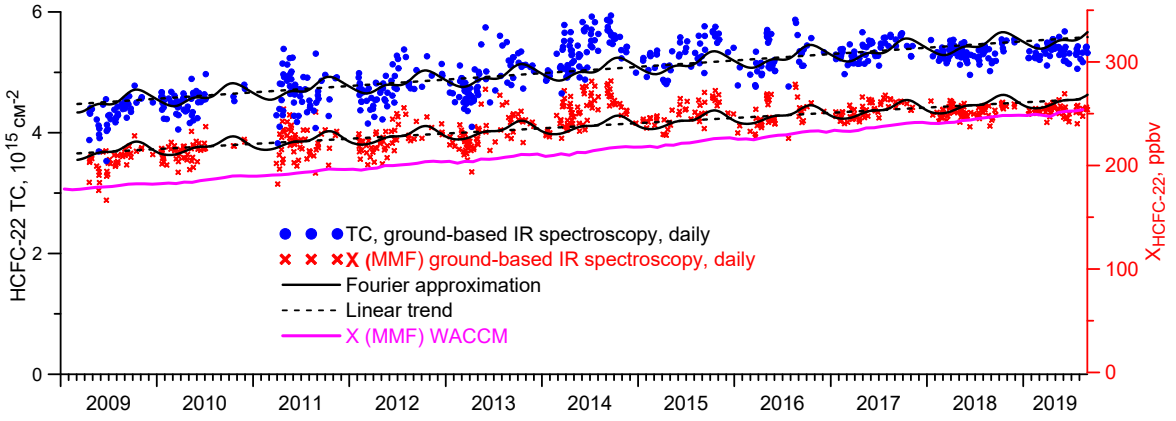

Figure 7. Daily mean TCs and MMFs of HCFC-22. Filtered results, T-Ph parameter $\alpha = 3 \times 10^3$.

3.3 Comparison with independent data

We compare the FTIR results at the St. Petersburg site with the data of independent measurements and modeling. There are no available experiments that are fully consistent with our FTIR measurements in space and time, so we try to find the closest possible data. There are three sources of data on the concentration of the freons in the atmosphere. First source – the in situ measurements at the surface (carried out by exactly in situ and the flask methods) are available from the AGAGE (Dunse et al., 2005) and HATS (Montzka et al., 1993) observational networks, data are regularly updated at ftp://ftp.cmdl.noaa.gov/hats/hcfcs/hcfc22/flasks/. Measurements are carried out at the fixed locations, the closest of which is Mace Head, Ireland (MHD) at a distance of $2500\,\mathrm{km}$ and $6.6°$ south of the St. Petersburg site. The mean values and the trends of the MMFs are calculated from the FTIR data and from the MHD site near–ground data for the period (2009–2019) for all three considered gases. The results are shown in Table 6 in columns 1 and 3. The mean near–ground VMRs (GVMRs) at the MHD site for CFC-11, CFC-12, and HCFC-22 equal 234, 517, and $237\,\mathrm{pptv}$, whereas the FTIR MMFs measurements show 225, 493, and $252\,\mathrm{pptv}$ means, respectively. The trend values (Table 6, columns 2, 4) for the GVMR data are -0.53, -0.59, $2.0\,\%\,\mathrm{yr}^{-1}$, for the FTIR data are -0.38, -0.48,

https://doi.org/10.5194/amt-2020-348
Preprint. Discussion started: 17 October 2020


Atmospheric Measurement Techniques Discussions

$2.0\,\%\,\mathrm{yr}^{-1}$ for CFC-11, CFC-12, and HCFC-22, respectively. Taking into account the spatial discrepancy, the different nature of the measured quantities, and different measurement conditions (background conditions on the Atlantic coast and measurements near the large agglomeration of St. Petersburg), the agreement between the mean values and the trends can be considered satisfactory. It should be noted that the differences in trend estimates do not go beyond the differences in trend values obtained by other researchers. Zhou et al. (2016) have obtained trends of -0.86, -0.76, $2.84\,\%\,\mathrm{yr}^{-1}$ for the period 2009–2016; the WMO (2018) indicated that averaged VMRs for 2015 comprised for $229.2-231.1$, $515.3-519.7$, $233.0-238.0\,\mathrm{pptv}$ and the trends for the period 2010–2016 were -0.70, -0.47, $2.54\,\%\,\mathrm{yr}^{-1}$ for CFC-11, CFC-12, and HCFC-22, respectively. Taking into account the decrease in both the rate of decay of CFC-11 and the rate of growth of HCFC-22 (e.g. Polyakov et al., 2020b), the agreement of both concentrations and trend values seems to be satisfactory.

The second source of information on the freons content is the satellite measurements, most fully with respect to the considered gases presented by the ACE–FTS instrument data which version 4 is described by Boone et al. (2020). The ACE–FTS is a high spectral resolution ($0.02\,\mathrm{cm}^{-1}$) Fourier transform spectrometer operating from 2.2 to $13.3\,\mu\mathrm{m}$ ($750-4400\,\mathrm{cm}^{-1}$) based on a Michelson interferometer. The instrument is a main payload onboard SCISAT–1 satellite with drifting orbit, inclination $73.9°$, and altitude $750\,\mathrm{km}$. Working primarily in solar occultation mode, the satellite provides vertical profile information (typically $10-100\,\mathrm{km}$) for temperature, pressure, and the VMRs of dozens of atmospheric gases over latitudes $85°\,\mathrm{N}$ to $85°\,\mathrm{S}$. The lower boundary of the retrieved profiles does not fall below $6\,\mathrm{km}$, but, as a rule, is above $7-8\,\mathrm{km}$, and the errors at the lower level may be greater than in the rest of the profile. Therefore, we use for comparisons only the profiles in which the data are available above $7\,\mathrm{km}$ and analyze the average satellite VMRs (SVMR) in the $8-12\,\mathrm{km}$ layer to reduce the random error. For comparison, we select the ACE–FTS measurements closer than $500\,\mathrm{km}$ from the St. Petersburg site. In 2009–2019, there are only 47 days of the SVMR measurements for CFC-11 (mean $233\,\mathrm{pptv}$, trend $-0.68\pm0.23\%\,\mathrm{yr}^{-1}$), 47 days for CFC-12 (mean $521\,\mathrm{ppyv}$, trend $-0.52\pm0.16\,\%\,\mathrm{yr}^{-1}$), and 46 days for HCFC-22 ($\mathrm{mean}240\,\mathrm{pptv}$, trend $2.0\pm0.5\,\%\,\mathrm{yr}^{-1}$). The results are shown in columns 7 and 8 of Table 6. Due to the peculiarity of the orbit and the weather conditions at the St. Petersurg site SCISAT–1 measurements are available on rare occasions; during 10 years we have found not more than 47 measurements closer than $500\,\mathrm{km}$ from the St. Petersburg site. However, the $95\,\%$ probability intervals show reliability of the trend estimates using the bootstrap method by Gardiner et al. (2008). As one can see by comparing columns 1 and 7 of Table 6, the confidence intervals of the means overlap, i.e. the difference in the mean values is not significant only for HCFC-22, and for both CFC-11 and CFC-12, the SVMR is significantly greater than the FTIR MMFs, the difference totals $8\,\mathrm{pptv}$, or $3.5\,\%$ for CFC-11 and $28\,\mathrm{pptv}$ or $6.3\,\%$ for CFC-12. To increase the number of data pairs, we analyze all ACE–FTS data at all longitudes in the $55-65°\,\mathrm{N}$ latitudinal belt including the St. Petersburg site (about $60°\,\mathrm{N}$). For the period of the FTIR measurements, the SVMR data contains 1113 measurements for CFC-11, with a mean of $235.3\,\mathrm{pptv}$ and a trend value of $-0.63\,\%\,\mathrm{yr}^{-1}$, 1120 measurements for CFC-12 ($526.4\,\mathrm{pptv}, -0.58\,\%\,\mathrm{yr}^{-1}$), and 1111 measurements for HCFC-22 ($239.5\,\mathrm{pptv}, 2.2\,\%\,\mathrm{yr}^{-1}$), see columns 5 and 6 of Table 6.

https://doi.org/10.5194/amt-2020-348
Preprint. Discussion started: 17 October 2020

Atmospheric Measurement Techniques Discussions

Table 6. The means and the trends estimates of the FTIR MMF, GVMR and SVMR measurements, and the WACCM MMFs. If the width of the confidence interval is not specified, it is less than the last significant digit.

Gas	IR spectroscopy, St. Petersburg, MMF		Mace Head, Ireland, GVMR		SCISAT, mean VMR $8\text{˘}12\,\mathrm{km}$, SVMR 55–65°N		SCISAT, mean VMR $8\text{˘}12\,\mathrm{km}$, SVMR Distance < $500\mathrm{km}$		WACCM, WMMF St. Petersburg	
	Mean, pptv	Trend, $\%\,\mathrm{yr}^{-1}$	Mean, pptv	Trend, $\%\,\mathrm{yr}^{-1}$	Mean, pptv	Trend, $\%\,\mathrm{yr}^{-1}$	Mean, pptv	Trend, $\%\,\mathrm{yr}^{-1}$	Mean, pptv	Trend $\%\,\mathrm{yr}^{-1}$
	1	2	3	4	5	6	7	8	9	10
CFC-11	225	-0.40 ± 0.07	234	-0.53 ± 0.02	235	-0.63	233 ± 3	-0.68 ± 0.23	203 ± 2	-1.68 ± 0.06
CFC-12	493 ± 1	-0.49 ± 0.04	517	-0.59 ± 0.01	526	-0.58	521 ± 4	-0.52 ± 0.16	478 ± 2	-0.84 ± 0.03
HCFC-22	238	2.12 ± 0.13	237	2.0 ± 0.05	240	2.2	240 ± 7	2.0 ± 0.5	215 ± 4	3.40 ± 0.03

With a 20 times larger dataset, the confidence intervals for the trends for the latitudinal belt are much narrower than for a circle with a radius of $500\,\mathrm{km}$, thus the differences in the SVMR trends vs FTIR MMF trends for CFC-11 and CFC-12 become significant. Such discrepancy may be due to the different physical nature of the compared quantities. The satellite data does not take into account the lower tropospheric layers where the influence of anthropogenic pollution sources is the greatest. Therefore, analyzing the trends and proceeding from this that the background values of the VMRs for atmospheric CFC-11 and CFC-12 (in situ and satellite) are falling faster than the FTIR MMFs in the industrially developed European part of Russia (near megacity St. Petersburg), we can conclude that some sources of CFC-11 and CFC-12 exist somewhere there. The absolute values of CFC-11 and CFC-12 FTIR MMFs are smaller than that of the in situ and satellite measurements, but this may only be due to the uncertainty of the used spectroscopy, see the estimates of the systematic in Table 4, row 10.

Figure 8 depicts the seasonal variation functions S (t), Eq. (4), for three gases and for four types of data: near–ground VMR at the MHD station (GVMR), satellite mean VMR $8-12\,\mathrm{km},\ 55-65°\,\mathrm{N}$ (SVMR), the MMFs by FTIR measurements (MMF), and the MMFs from the WACCM (WMMF). Figure 8 demonstrates the low seasonal variability of the GVMR – within tenths of a per cent for CFC-11 and CFC-12 and within $0.7\,\%$ for HCFC-22. At the same time, a noticeable seasonal variations of the FTIR MMFs and the SVMR values for all three gases and of the WACCM MMFs for CFC-11 and CFC-12 are observed. The maximum amplitude of the variability for CFC-11 reaches $4\,\%$, for HCFC-22 slightly exceeds $3\,\%$, and for CFC-12 is close to $2\,\%$. For all three gases, the seasonal variations of the SVMR and the MMFs are qualitatively and quantitatively similar: in spring (March–April) there is a minimum, and in late summer or autumn (August–October) is a maximum. At the same time, there are some differences in the seasonal cycles: for CFC-11, the change in the MMFs is 2-3 months ahead of the SVMR, while for HCFC-22 the autumn maximum shows the same tendency, whereas the spring minimum, on the contrary, is observed simultaneously for the MMFs and the SVMR. For CFC-12, the MMFs amplitude is approximately half that for the two other gases; the spring minimum of the MMFs, on the contrary, is observed before that of the SVMR, and the autumn maxima are coincided. For CFC-12, a second maximum in the MMFs seasonal cycle is observed in the early summer. The WMMF for CFC-11 and CFC-12 in a whole show a qualitatively and quantitatively similar character of seasonal variability to the MMFs

https://doi.org/10.5194/amt-2020-348
Preprint. Discussion started: 17 October 2020

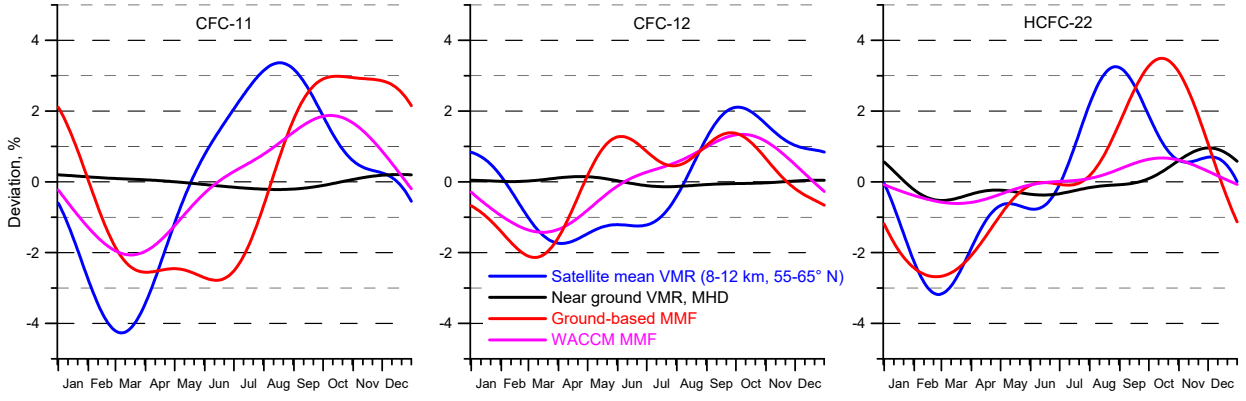

Figure 8. Seasonal relative variability of CFC-11 (left), CFC-12 (center), and HCFC-22 (right). Satellite refer to the ACE-FTS measurements, ground-based and WACCM refer to the FTIR measurements and numerical modeling at the St. Petersburg site.

and the SVMR, while for HCFC-22, on the contrary, the changes in the WMMF are significantly less (less than 1 %) than that of the MMFs and the SVMR. In general, we can conclude that the MMFs, SVMR, and WMMF show qualitative similar seasonal variation with some quantitative differences, and the GVMR variabilities are significantly less. The variability of the WMMF for HCFC-22 only depicts the exception, it is essentially less than the MMFs and SVMR variability.

4 Conclusions

1. The retrieval strategies for deriving the TCs of CFC-11, CFC-12, and HCFC-22 using ground-based IR solar spectra measurements by Bruker IFS125HR spectrometer have been improved. The T–Ph approach is applied to solving the inverse problem as it is more suitable for long–lived gases with noticeable trends than the OE regularization. The values of the regularization

https://doi.org/10.5194/amt-2020-348
Preprint. Discussion started: 17 October 2020


Atmospheric Measurement Techniques Discussions

parameter are optimized. For the FTIR measurements over the NDACC site St. Petersburg in 2009–2019, the estimates of the DFS values are 1.05 ± 0.06, 1.20 ± 0.05, 1.00 ± 0.00, the estimates of the relative systematic and random errors are $7.61\,\%$ and $3.08\,\%$, $2.24\,\%$ and $2.40\,\%$, and $5.75\,\%$ and $3.70\,\%$, for CFC-11, CFC-12,and HCFC-22, respectively.

2. The time series of the TCs and MMFs of CFC-11, CFC-12, and HCFC-22 above the St. Petersburg site near Saint-Petersburg, Russia in 2009–2019 have been obtained. Mean values of the MMFs of CFC-11, CFC-12, and HCFC-22 are 225, 493, and $238\,\mathrm{pptv}$. The RMS daily variability of the TCs of measured gases are 0.8, 0.6, $2.3\,\%$ for three gases in the same order. Estimates of the MMFs trends of CFC-11, CFC-12, and HCFC-22 equal $-0.40 \pm 0.07\,\%\,\mathrm{yr}^{-1}$, $-0.49 \pm 0.05\,\%\,\mathrm{yr}^{-1}$, and $2.12 \pm 0.13\,\%\,\mathrm{yr}^{-1}$, respectively. The analysis of the seasonal variability of CFC-11, CFC-12, and HCFC-22 demonstrates the similar qualititaive seasonal variability for all three gases with minimum in spring–begin of summer and maximum in fall; the MMFs variability of CFC-11 and HCFC-22 amounts to $3\,\%$, the MMFs variability of CFC-12 amounts to $2\,\%$.

3. Mean values, trends and seasonal variability of CFC-11, CFC-12, and HCFC-22 MMFs above St. Petersburg site are compared to the same parameters of the near ground VMRs measured at the site Mace Head, Ireland. It is shown that the mean of the CFC-11 MMFs above St. Petersburg site is $9\,\mathrm{pptv}(3.8\,\%)$ less than the mean GVMR at MSH site, the mean of the CFC-12 MMFs is $24\,\mathrm{pptv}(4.6\,\%)$ less than the mean GVMR, and the mean of the HCFC-22 MMFs does not significantly differ from the mean GVMR. In ablolute values, the trend of the CFC-11 MMFs is $0.13\,\%\,\mathrm{yr}^{-1}$ less (-0.40 vs $-0.53\,\%\,\mathrm{yr}^{-1}$), the trend of the CFC-12 MMFs is $0.10\,\%\,\mathrm{yr}^{-1}$ less (-0.49 vs $-0.59\,\%\,\mathrm{yr}^{-1}$) than that of the GVMR, and the trend of the HCFC-22 MMFs does not significantly diff from that of the GVMR ($2.12 \pm 0.13\,\%\,\mathrm{yr}^{-1}$ vs $2.0 \pm 0.05\,\%\,\mathrm{yr}^{-1}$). The seasonal variability of the GVMR for all three gases is much lower than the MMFs variability.

4. Mean values, trends and seasonal variability of CFC-11, CFC-12, and HCFC-22 MMFs above St. Petersburg site are compared to the same parameters of the SVMR. The SVMR stands for the mean values of VMR, measured with ACE–FTS between altitudes $8 - 12\,\mathrm{km}$ and between latitudes $55 - 65°\,\mathrm{N}$. It is shown that the mean CFC-11 MMFs is $10\,\mathrm{pptv}(4.3\,\%)$ less than the mean SVMR, the mean CFC-12 MMFs is $33\,\mathrm{pptv}(6.3\,\%)$ less than the mean SVMR, and the mean HCFC-22 MMFs is $2\,\mathrm{pptv}(0.8\,\%)$ less than the mean SVMR. In absolute value, the CFC-11 MMFs trend is $0.23\,\%\,\mathrm{yr}^{-1}$ less ($-0.40\,\mathrm{vs}\,-0.63\,\%\,\mathrm{yr}^{-1}$) than the trend of the SVMR, the trend of CFC-12 MMFs is $0.09\,\%\,\mathrm{yr}^{-1}$ less than the trend of the SVMR ($-0.49\,\mathrm{vs}\,-0.58\,\%\,\mathrm{yr}^{-1}$), and the trend of HCFC-22 MMFs does not significantly differ from that of the SVMR (2.12 ± 0.13 vs $2.2\,\%\,\mathrm{yr}^{-1}$). The MMFs and SVMR show qualitative and quantitative similar seasonal variation.

5. Mean values, trends and seasonal variability of CFC-11, CFC-12, and HCFC-22 MMFs are compared to the same parameters of the WMMF. The WMMF stands for the MMFs calculated on the basis of the WACCM dataset of the VMR profiles for the St. Petersburg site. It is shown that the mean CFC-11 MMFs is $22\,\mathrm{pptv}\,(10\,\%)$ greater than the mean WMMF, the mean CFC-12 MMFs is $15\,\mathrm{pptv}\,(3.1\,\%)$ greater than the mean WMMF, and the mean HCFC-22 MMFs is $23\,\mathrm{pptv}\,(10\,\%)$ greater than the mean WMMF. In absolute value, the CFC-11 MMFs trend is $1.28\,\%\,\mathrm{yr}^{-1}$ less than the trend of the WMMF (-0.40 vs $-1.68\,\%\,\mathrm{yr}^{-1}$), the trend of the CFC-12 MMFs is $0.35\,\%\,\mathrm{yr}^{-1}$ less than the trend of the WMMF (-0.49 vs $-0.84\,\%\,\mathrm{yr}^{-1}$), and the trend of the HCFC-22 MMFs is $1.28\,\%\,\mathrm{yr}^{-1}$ less than the trend of the WMMF ($2.12\,\%\,\mathrm{yr}^{-1}$ vs $3.40\,\%\,\mathrm{yr}^{-1}$). The MMFs and WMMF show qualitative and quantitative similar seasonal variations for CFC-11 and CFC-12; the seasonal variability of the WMMF for HCFC-22 is essentially less than the MMF variability.

https://doi.org/10.5194/amt-2020-348
Preprint. Discussion started: 17 October 2020


Atmospheric Measurement Techniques Discussions

In general, the comparison of the FTIR MMFs with the independent data shows a good agreement of their means within the systematic error of the measurements. The observed trends over the St. Petersburg site demonstrate the smaller decrease rates for CFC-11 and CFC-12 than the independent data, and the same decrease rate for HCFC-22. The suggested retrieval strategies can be used for analysis of the IR solar spectra measurements using Bruker FS125HR spectrometers, e.g. at other sites of the NDACC observational network.

Data availability. The FTIR CFC-11, CFC-12 and HCFC-22 retrievals at St Petersburg are available from NDACC (http://www.ndaccdemo.org/data). The MHD HATS CFC-11, CFC-12, and HCFC-22 data are publicly available from NOAA (http://www.esrl.noaa.gov/gmd/hats. SCISAT-1 ACE-FTS data version 4.1 can be asked from ACE-FTS group (http://www.ace.uwaterloo.ca/data.php). WACCM profiles at St. Petersburg site are available from IRWG NDACC (https://www2.acom.ucar.edu/irwg/links).

Author contributions. APol Conceptualization, Data curation, Formal analysis, Funding acquisition, Investigation, Methodology, Project administration, Resources, Software, Validation, Visualization, Writing – original draft. APob Investigation (performed measurements of spectral sensitivity functions, and was responsible for the measurements of solar radiation), Conceptualization (detected the effects of cryo–sediment). MM Investigation (was responsible for the measurements of solar radiation), Resources, Writing – review and editing. YV Investigation (the water vapor profiles), Writing – review and editing. YM Conceptualization (originally proposed a general research topic).

Competing interests. The authors declare that they have no conflict of interest.

Acknowledgements. This work was supported by Russian Foundation for Basic Research, grant 18–05–00426. The ACE mission is funded by the Canadian Space Agency. NOAA data were provided by S. Montzka, 2019. We thank J. W. Hannigan (NCAR, Boulder, CO, USA) for providing the data of the WACCM model at the NDACC station in St. Petersburg. The ground–based TCs measurements of solar radiation at St. Petersburg site were obtained using the equipment of the SPbU "Geomodel" Resource Center.

https://doi.org/10.5194/amt-2020-348
Preprint. Discussion started: 17 October 2020

Atmospheric Measurement Techniques Discussions

References

Boone, C. D., Bernath, P. F., Cok, D., Jones, S. C., Steffen, J.: Version 4 retrievals for the atmospheric chemistry experiment Fourier transform spectrometer (ACE–FTS) and imagers, J. Quant. Spectrosc. Ra., 247, 106939, https://doi.org/10.1016/j.jqsrt.2020.106939, 2020.

Brown, A. T., Chipperfield, M. P., Boone, C., Wilson, C., Walker, K. A., Bernath, P. F.: Trends in atmospheric halogen containing gases since 2004, J. Quant. Spectrosc. Ra., 112, 2552—2566, https://doi.org/10.1016/j.jqsrt.2011.07.005, 2011.

Cracknell, A. P., and Varotsos, C. A.: The contribution of remote sensing to the implementation of the Montreal Protocol and the monitoring of its success, Int. J. Remote Sens., 30(15–16), 3853–3873, https://doi.org/10.1080/01431160902821999, 2009.

Dunse, B. L., Steele, V., Wilson, S. R., Fraser, P. J., Krummel, P. B.: Trace gas emissions from Melbourne, Australia, based on AGAGE observations at Cape Grim, Tasmania, 1995–2000, Atmos. Environ. 39(34), 6334–6344, doi.org/10.1016/j.atmosenv.2005.07.014, 2005.

Eckert, E., Laeng, A. , Lossow, S. , Kellmann, S., Stiller, G., von Clarmann, T., Glatthor, N., Höpfner, M., Kiefer, M., Oelhaf, H., Orphal, J., Funke, B., Grabowski, U., Haenel, F., Linden, A., Wetzel, G., Woiwode, W., Bernath, P. F., Boone, C., Dutton, G. S., Elkins, J. W., Engel, A., Gille, J. C., Kolonjari, F., Sugita, T., Toon, G. C., Walker, K. A.: MIPAS IMK/IAA CFC-11 (CCl3F) and CFC-12 (CCl2F2) measurements: accuracy, precision and long-term stability, Atmos. Meas. Tech., 9, 3355—3389, https://doi.org/10.5194/amt-9-3355-2016, 2016.

Gardiner, T., Forbes, A., de Mazière, M., Vigouroux, C., Mahieu, E., Demoulin, P., Velazco, V., Notholt, J., Blumenstock, T., Hase, F., Kramer, I., Sussmann, R., Stremme, W., Mellqvist, J., Strandberg, A., Ellingsen, K., and Gauss, M.: Trend analysis of greenhouse gases over Europe measured by a network of ground–based remote FTIR instruments, Atmos. Chem. Phys., 8, 6719–6727, https://doi.org/10.5194/acp-8-6719-2008, 2008.

Hase, F., Hannigan, J. W., Coffey, M. T., Goldman, A., Höpfner, M., Jones, N. B., Rinsland, C. P., Wood, S. W.: Intercomparison of retrieval codes used for the analysis of high–resolution, ground–based FTIR measurements, J. Quant. Spectrosc. Ra., 87, 25—52, 2004.

Hoffmann, L. and Riese, M.: Quantitative transport studies based on trace gas assimilation, Adv. Space Res., 33, 1068–1072, doi:10.1016/S0273-1177(03)00592-1, 2004

Hoffmann, L., Kaufmann, M., Spang. R., Müller, R., Remedios, J. J., Moore, D. P., Volk, C. M., von Clarmann, T., Riese, M.: Envisat MIPAS measurements of CFC-11: retrieval, validation, and climatology, Atm. Chem. Phys., 8, 3671—3688, https://acp.copernicus.org/articles/8/3671/2008/acp-8-3671-2008.pdf, 2008.

Hudgins, D. M., Sandford, S. A., Allamandola, L. J., Tielens, A. G. G. M.: Mid- and Far-Infrared Spectroscopy of Ices: Optical Constants and Integrated Absorbances, Astrophys. J. Suppl. S., 86, 713—870, DOI 10.1086/191796, 1993.

Kellmann, S., von Clarmann, T., Stiller, G. P., Eckert, E., Glatthor, N., Höpfner, M., Kiefer, M., Orphal, J., Funke, B., Grabowski, U., Linden, A., Dutton, G. S., and Elkins, J. W.: Global CFC-11 (CCl3F) and CFC-12 (CCl2F2) measurements with the Michelson Interferometer for Passive Atmospheric Sounding (MIPAS): retrieval, climatologies and trends, Atmos. Chem. Phys., 12, 11857–11875, https://doi.org/10.5194/acp-12-11857-2012, 2012.

Khosrawi, F., Müller, R., Irie, H., Engel, A., Toon, G., Sen, B., Aoki, S., Nakazawa, T., Traub, W.,Jucks, K. J.: Validation of CFC-12 measurements from the Improved Limb Atmospheric Spectrometer (ILAS) with the version 6.0 retrieval algorithm, J. Geophys. Res.–Atmos., 109, D06311, https://doi.org/10.1029/2003JD004325, 2004

Lynch, D. K.: The Infrared Spectral Signature of Water Ice in the Vacuum Cryogenic AI&T Environment, Report No. TR-2006(8570)-1, (Approved for public release; distribution unlimited), The Aerospace Corporation Laboratory Operations, 2450 E. El Segundo Blvd. 11., Los Angeles Air Force Base, CA 90245, 19pp, 2006.

https://doi.org/10.5194/amt-2020-348
Preprint. Discussion started: 17 October 2020

Mahieu, E., O'Doherty, S., Reimann, S., Vollmer, M., Bader, W., Bovy, B., Lejeune, B., Demoulin, P., Roland G., Servais, C.: First retrievals of HCFC-142b from ground-based high-resolution FTIR solar observations: application to high–altitude Jungfraujoch spectra, Geophys. Res. Abstr., 15, EGU2013-1185-1, https://meetingorganizer.copernicus.org/EGU2013/EGU2013-1185.pdf, 2013.

Mahieu, E., Duchatelet, P., Demoulin, P., Walker, K. A., Dupuy, E., Froidevaux, L., Randall, C., Catoire, V., Strong, K., Boone, C. D., Bernath, P. F., Blavier, J.-F., Blumenstock, T., Coffey, M., de Mazière, M., Griffith, D., Hannigan, J., Hase, F., Jones, N., Jucks, K. W., Kagawa, A., Kasai, Y., Mebarki, Y., Mikuteit, S., Nassar, R., Notholt, J., Rinsland, C. P., Robert, C., Schrems, O., Senten, C., Smale, D., Taylor, J., T?tard, C., Toon, G. C., Warneke, T., Wood, S. W., Zander, R., and Servais, C.: Validation of ACE–FTS v2.2 measurements of HCl, HF, CCl3F and CCl2F2 using space-, balloon- and ground-based instrument observations, Atmos. Chem. Phys., 8, 6199–6221, https://doi.org/10.5194/acp-8-6199-2008, 2008.

Mahieu, E., Lejeune, B., Bovy, B., Servais, C., Toon, G. C., Bernath, P. F., Boone, C. D., Walker, K. A., Reimann, S., Vollmer, M. K., Retrieval of HCFC-142b (CH3CClF2) from ground–based high–resolution infrared solar spectra: Atmospheric increase since 1989 and comparison with surface and satellite measurements, J. Quant. Spectrosc. Ra., 186, 96—105, 2017.

Mahieu, E., Rinsland, C. P., Gardiner, T., Zander, R., Demoulin, P., Chipperfield, M. P., Ruhnke, R., Chiou, L. S., De Mazière, M., and the GIRPAS Team: Recent trends of inorganic chlorine and halogenated source gases abovethe Jungfraujoch and Kitt Peak stations derived from high–resolution FTIR solar observations, Geophys. Res. Abstr., 12, EGU2010-2420-3, https://meetingorganizer.copernicus.org/EGU2010/EGU2010-2420-3.pdf, 2010.

Mlawer, E. J., Payne, V. H., Moncet, J. L., Delamere, J. S., Alvarado, M. J., Tobin, D. D.: Development and recent evaluation of the MT_CKD model of continuum absorption, Philos. T. r. soc. A, 370, 1—37, https://doi.org/10.1098/rsta.2011.0295, 2012.

Continuum Model MT_CKD_3.2, http://rtweb.aer.com/continuum_code.html, 2017

Molina, M., Rowland, F.: Stratospheric sink for chlorofluoromethanes: chlorine atom–catalysed destruction of ozone, Nature, 249, 810–812, https://doi.org/10.1038/249810a0, 1974.

Montzka, S. A., Dutton, G. S., Yu, P., Ray, E., Portmann, R. W., Daniel J. S., Kuijpers, L., Hall, B. D., Mondeel, D., Siso, C., Nance, J. D., Rigby, M., Manning, A. J., Hu, L., Moore, F., Miller, B. R., Elkins, J. W.: An unexpected and persistent increase in global emissions of ozone–depleting CFC-11, Nature, 557, 413—417, https://doi.org/10.1038/s41586-018-0106-2, 2018.

Montzka, S. A., Myers, R. C., Butler, J. H., Elkins, J. W., Cummings, S. O.: Geophys. Research Lett., 20(8), 703—706, doi:10.1029/93GL00753, 1993. data are regularly updated at ftp://ftp.cmdl.noaa.gov/hats/hcfcs/hcfc22/flasks/

Notholt, J.: FTIR measurements of HF, N2O and CFCs during the Arctic polar night with the Moon as light source, subsidence during winter 1992/93, Geophys. Res. Lett., 21, 2385—2388, https://doi.org/10.1029/94GL02351, 1994.

Park, M., Randel, W. J., Kinnison, D. E., Emmons, L. K., Bernath, P. F., Walker, K. A., Boone, C. D., Livesey, M. J.: Hydrocarbons in the upper troposphere and lower stratosphere observed from ACE–FTS and comparisons with WACCM, J. Geophys. Res.–Atmos., 118(4), 1964—1980, https://doi.org/10.1029/2012JD018327, 2013.

Phillips, D.: A technique for the numerical solution of certain integral equations of the first kind, J. ACM, 9 (1), 84–97, doi:10.1145/321105.321114, 1962.

Polyakov, A. V., Poberovsky, A. V., Virolainen, Y. A., Makarova M. V.: Transparency Spectra Inversion Technique for Evaluating the Atmospheric Content of CCl3F freon, J. Appl. Spectrosc., 87, 92–98, https://doi.org/10.1007/s10812-020-00968-6, 2020a.

Polyakov, A. V., Timofeyev, Y. M., Virolainen, Y. A., Makarova, M. V., Poberovskii, A. V., & Imhasin, H. K.: Ground–Based Measurements of the Total Column of Freons in the Atmosphere near St. Petersburg (2009–2017), Izv. AN phys. Atmos. Oc., 54, 487–494, https://doi.org/10.1134/S0001433818050109, 2018.

https://doi.org/10.5194/amt-2020-348
Preprint. Discussion started: 17 October 2020

Atmospheric Measurement Techniques Discussions

Polyakov, A. V., Virolainen, Y. A., & Makarova, M. V.: Technique for Inverting Transmission Spectra to Measure Freon Concentration, J. Appl. Spectrosc., 85(6), 1085–1093, https://doi.org/10.1007/s10812-019-00763-y, 2019a.

Polyakov, A. V., Virolainen, Y. A., & Makarova M. V.: Method For Inversion Of The Transparency Spectra For Evaluating The Content of CCl2F2 In The Atmosphere, J. Appl. Spectrosc., 86(3), 449–456, https://doi.org/10.1007/s10812-019-00840-2, 2019b.

Polyakov, A., Virolainen, Y., Poberovskiy, A., Makarova, M., & Timofeyev, Y.: Atmospheric HCFC-22 total columns near St. Petersburg: stabilization with start of a decrease, Int. J. Rem. Sens., 41(11), 4365–4371, https://doi.org/10.1080/01431161.2020.1717668, 2020b.

Prignon, M., Chabrillat, S., Minganti, D., O'Doherty, S.: Improved FTIR retrieval strategy for HCFC-22 (CHClF2), comparisons with in situ and satellite datasets with the support of models, and determination of its long–term trend above Jungfraujoch, Atmos. Chem. Phys., 19, 12309–12324, https://doi.org/10.5194/acp-19-12309-2019, 2019.

Rodgers, C. D.: Inverse Meyhods for Atmospheric Sounding: Theory and Practice, Series on Atmospheric, Oceanic and Planetary Physics: Volume 2, World Scientific Publishing, PO Box 128, Farrer road, Singapore, 912805, 238pp, https://doi.org/10.1142/3171, 2000.

Rodgers, C. D., and Connor, B. J.: Intercomparison of remote sounding instruments, J. Geophys. Res,, 108(D3), 4116, doi:10.1029/2002JD002299, 2003.

Sussmann, R., Forster, F., Rettinger, M., and Jones, N.: Strategy for high–accuracy–and–precision retrieval of atmospheric methane from the mid–infrared FTIR network, Atmos. Meas. Tech., 4, 1943–1964, doi:10.5194/amt-4-1943-2011, 2011.

Tikhonov, A., On the solution of incorrectly stated problems and a method of regularization, Dokl. Akad. Nauk SSSR, 151, 501–504, 1963.

Timofeev, Yu. M., Polyakov, A. V., Virolainen, Ya. A., Makarova, M. V., Ionov, D. V., Poberovsky, A. V., Imhasin, H. H.: Estimates of Trends of Climatically Important Atmospheric Gases Near St. Petersburg, Izv. AN phys. Atmos. Oc., 56,(1), 79–84, 2020b.

Timofeyev Yu., Virolainen, Ya., Makarova, M., Poberovsky, A., Polyakov, A., Ionov, D., Osipov, S., Imhasin, H.: Ground–based spectroscopic measurements of atmospheric gas composition near Saint Petersburg (Russia), J. Mol. Spectr., 323, 2—14, 2016.

Virolainen, Y. A., Timofeyev, Y. M., Kostsov, V. S., Ionov, D. V., Kalinnikov, V. V., Makarova, M. V., Poberovsky, A. V., Zaitsev, N. A., Imhasin, H. H., Polyakov, A. V., Schneider, M., Hase, F., Barthlott, S., and Blumenstock, T.: Quality assessment of integrated water vapour measurements at the St. Petersburg site, Russia: FTIR vs. MW and GPS techniques, Atmos. Meas. Tech., 10, 4521–4536, https://doi.org/10.5194/amt-10-4521-2017, 2017.

WMO (World Meteorological Organization), Scientific Assessment of Ozone Depletion: 2018, Global Ozone Research and Monitoring Project–Report No. 58, 588, Geneva, Switzerland, 2018.

Yagovkina, I. S., Polyakov, A. V., Poberovskii, A. V., Timofeyev Yu. M.: Spectroscopic measurements of total CFC-11 freon in the atmosphere near St. Petersburg, Izv. AN phys. Atmos. Oc., 47, 186–189, https://doi.org/10.1134/S0001433811020125, 2011.

Zander, R., Mahieu, E., Demoulin, P., Duchatelet, P., Servais, C., Roland, G., Delbouille, L., De Mazière, M., and Rinsland, C.P.: Evolution of a dozen non–CO2 greenhouse gases above Central Europe since the mid–1980s, Environ. Sci., 2, 295–303, doi:10.1080/15693430500397152, 2005.

Zhou, M., Vigouroux, C., Langerock, B., Wang, P., Dutton, G., Hermans, C., Kumps, N., Metzger, J. M., Toon, G., and De Mazière, M.: CFC-11, CFC-12 and HCFC-22 ground-based remote sensing FTIR measurements at Réunion Island and comparisons with MIPAS/ENVISAT data, Atmos. Meas. Tech., 9, 5621–5636, https://doi.org/10.5194/amt-9-5621-2016, 2016.